

# Stark effect in colloidal indium arsenide nanocrystal quantum dots: consequences for wave function mapping experiments

Michael Tews and Daniela Pfannkuche

*I. Institute of Theoretical Physics, University of Hamburg, Jungiusstr. 9, 20355 Hamburg, Germany*

The influence of the tip-substrate bias induced electric field in a scanning tunneling spectroscopy experiment on colloidal InAs nanocrystals has been studied. Calculating the Stark induced splitting of the degenerate  $1P_e$  state perturbatively within a particle-in-a-sphere model, revealed a possible explanation of recently published experimental wave function mapping data by Millo et al.<sup>1</sup>

## I. INTRODUCTION

Mapping of the electronic wave functions in semiconductor quantum dots (QD) has recently become possible using various experimental techniques<sup>1-3</sup>. Knowing the actual shape of the electronic densities contributes to a better understanding of the QD electronic structure. This knowledge is crucial with respect to the possible importance of semiconductor QDs as the ultimate building blocks of optoelectronic and nanoelectronic devices.

Most recent scanning tunneling microscopy (STM) measurements<sup>1</sup> also allow a wave function mapping of colloidal nanocrystals. The used InAs/ZnSe core/shell structures are spherical in shape resulting in atomic-like symmetries and degeneracies of the conduction band (CB) states<sup>4,5</sup>. This leads, for example, to a six fold degenerate first excited state (here after referred to as the  $1P_e$  state, where the subscription  $e$  denotes an electron rather than a hole state) such that a mapping of the  $1P_e$  wave function should reveal the spherical superposition of all degenerate states. In contrast to this simple prediction the experimental data<sup>1</sup> show a torus like  $p_{x^2+y^2}$  symmetry.

We present a calculation of the CB states within a particle-in-a-sphere model taking into account the electric field due to the applied STM voltage. The resulting quantum-confined Stark effect was studied earlier in three dimensional QDs<sup>6,7</sup>. In this work we concentrate on the Stark effect induced degeneracy lifting of the first excited state which provides an explanation for the observed  $p_{x^2+y^2}$  wave function symmetry<sup>1</sup> at appropriate STM voltages.

## II. MODEL

A sketch of the experimental setup in a scanning tunneling spectroscopy (STS) experiment on colloidal

nanocrystal quantum dots is shown in Fig. 1. To obtain a tunnel spectrum the tip is positioned above a single nanocrystal attached to the substrate via hexane dithiol molecules. Keeping the tip-cluster distance constant the differential conductance as a function of applied voltage shows sharp peaks<sup>4,8,9</sup>. For a detailed understanding of the experimental data it is thus crucial to know the discrete energetic spectrum of the QD since the obtained peak positions  $U_{peak}$  are directly related to the electronic dot structure<sup>9</sup>:

$$U_{peak}(N, N+1) = \gamma[E(N+1, \mu) - E(N, \nu)] \quad (1)$$

$$E(N, \mu = \{n_i\}) = \sum_i n_i \epsilon_i + V_Q^{tot}(\{n_i\}) \quad (2)$$

where the pre-factor  $\gamma$  depends on the capacitive electrostatic geometry. For a very asymmetric tip-dot dot-substrate capacity distribution  $\gamma$  is close to one<sup>9</sup>. The total energy  $E(N, \{n_i\})$  of a dot with  $N = \sum_i n_i$  electrons, where  $n_i$  denotes the occupation number of state  $i$ , is written as a sum of occupied single particle levels with energies  $\epsilon_i$  and the total charging energy  $V_Q^{tot}$ . Hereby  $V_Q^{tot}$  includes both, the direct Coulomb interaction and all correlations.

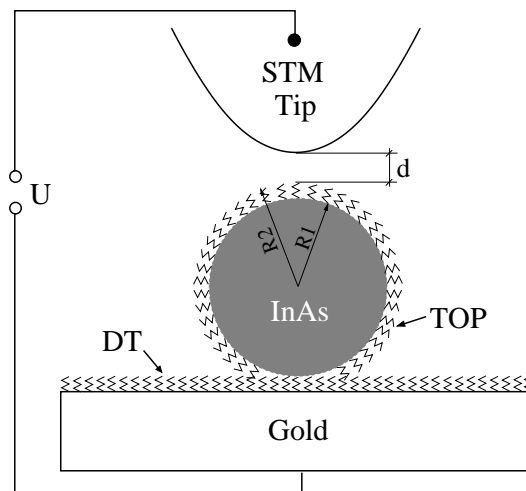


FIG. 1. Scanning tunneling spectroscopy of a single InAs nanocrystal. The InAs nanocrystal with a typical radius of a few nanometers are linked to a gold substrate by hexane dithiol molecules (DT). Trioctylphosphin (TOP) molecules form a ligand shell around the nanocrystal. At 4.2K the tunnel current is measured as a function of the applied voltage  $U$  between tip and substrate.

In the STS setup of Fig. 1 with voltages up to  $U \approx 2V^{1,4}$  applied on a tip-substrate distance of a few

nanometers, the QD is exposed to a considerable electric field. For simplicity we assume the field between tip and substrate to be homogeneous in the absence of the QD. Since the considered InAs clusters are surrounded by ligands with a quite different relative dielectric constant compared to InAs, we modeled the QD as a jacketed dielectric sphere. Extending the text book calculation of the electric potential  $\phi_{InAs}$  inside a dielectric sphere placed in a homogeneous field  $\varepsilon_{hom}$ <sup>10</sup> to such a structure leads in spherical coordinates to:

$$\phi_{InAs}(r, \theta) = \frac{9\epsilon_2\varepsilon_{hom}r\cos\theta}{2\epsilon_2^2 + \epsilon_1\epsilon_2 + 4\epsilon_2 + 2\epsilon_1 + 2(\frac{R_1}{R_2})^3[\epsilon_1\epsilon_2 + \epsilon_2 - \epsilon_1\epsilon_2^2]} \quad (3)$$

with  $\epsilon_1 = 15.15$ <sup>11</sup> and  $\epsilon_2 = 2.1$ <sup>12</sup> being the relative dielectric constants of InAs and the ligands respectively.  $R_1$  is the InAs core radius and  $R_2$  the total radius including the ligand shell (see Fig. 1). As in the case of a dielectric sphere without a shell<sup>10</sup> the core potential  $\phi_{InAs}$  is still the potential of a homogeneous field. The field  $\varepsilon_{hom}$  occurring in (3) is not directly accessible. It is obtained by equating the voltage  $U$  with the potential drop between tip and substrate of the inhomogeneous field outside the QD.

The single particle spectrum of conduction band (CB) states was calculated using a particle-in-a-sphere model with a finite potential well<sup>13</sup>. Such a spherical confinement leads to size quantization comparable to the bulk energy gap of InAs. Hence non-parabolicity effects of the CB have to be taken into account. We use an energy dependent effective mass approach<sup>14</sup> with

$$m^*(E) = m^*(0)[1 + E/E_g] \quad (4)$$

where  $m^*(0)$  is the bottom CB effective mass and  $E_g$  the bulk energy gap. The validity of this approach has been checked by Bryant<sup>15</sup> for a dot radius of 3.2 nm by comparison to a 8 band calculation including CB-valence band coupling.

Using the obtained electric potential inside the QD our model Hamiltonian is:

$$H = -\frac{\hbar^2}{2m^*(E)}\nabla^2 + V(r) - e\phi_{InAs}(r, \theta) \quad (5)$$

with  $V(r)$  being the potential step with step height corresponding to the work function of InAs towards air. The ligand shell is not included in the potential  $V(r)$ .

For calculating the QD states in the field we treated the electric potential perturbatively. The energies are obtained using second order perturbation theory<sup>16</sup>.

### III. RESULTS

Without an electric field the Hamiltonian (5) separates in an angular and a radial part. The angular Schrödinger

equation is solved by spherical harmonics, and the radial Schrödinger equation by spherical Bessel functions  $j_l$  inside the well and spherical Hankel functions  $h_l$  outside<sup>17</sup> the well. The continuity conditions at the potential step lead to a set of transcendental equation determining the energy levels:

$$\frac{\alpha j_{l-1}(\alpha R_1)}{j_l(\alpha R_1)} - (l+1)j_{l+1}(\alpha R_1) = \frac{i\beta h_{l-1}(i\beta R_1)}{h_l(i\beta R_1)} - (l+1)h_{l+1}(i\beta R_1) \quad (6)$$

with  $\alpha = \sqrt{2m^*E}/\hbar$  and  $\beta = \sqrt{2m^*(V-E)}/\hbar$ . The numerical solution of the first two energy levels for a dot radius of 3.2 nm is shown in Tab. I. Other than in hydrogen the allowed orbital quantum numbers are not restricted by the principal quantum number. Hence the first excited state has the quantum numbers  $n = 1$  and  $l = 1$ . Owing to the spherical harmonics this state is 3-fold degenerate in the three magnetic quantum numbers  $m = -1, 0$  and  $1$  (see Fig. 3 and 4). These unperturbed wave functions of (5) are now used to calculate the effect of the electric potential,  $\phi_{InAs}$  using second order perturbation theory.

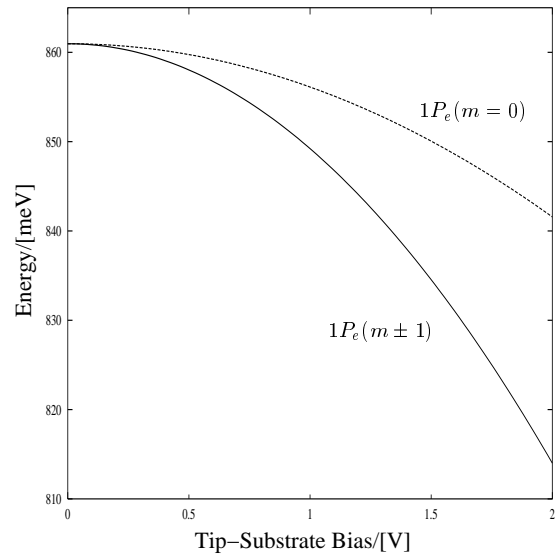


FIG. 2. Stark splitting of the  $1P_e$  level in a 3.2 nm radius InAs nanocrystal as a function of the applied tip-substrate voltage. For calculating the QD potential the ligand shell was taken to be  $R_2 - R_1 = 0.5$  nm thick whereas the tip-shell distance was taken as another  $d = 0.5$  nm (see Fig. 1). 3eV was used for the depth of the confining potential as obtained by<sup>18</sup> using a pseudopotential approach. To get the energy dependent mass, the InAs bulk energy gap  $E_g = 0.42$ eV<sup>11</sup> and the effective mass  $m^*(0) = 0.0239$ <sup>11</sup> in units of the free electron mass, were used.

Although the  $1S_e$  state also shows a Stark effect we concentrate here on the first excited  $1P_e$  state, with regard to the experimental results obtained by Millo et.

al.<sup>1</sup>. In contrast to hydrogen, the first excited state does not show a linear Stark effect, owing to the lack of s-p degeneracy in such a spherical well. The  $1P_e$  degeneracy is lifted by the quadratic Stark effect, such that the energy of the  $1P_e(m \pm 1)$  wave functions oriented perpendicular to the field (bottom row in Fig. 3) are lowered compared to the  $1P_e(m = 0)$  wave function oriented along the field (top row in Fig. 3). This behavior can be qualitatively understood by looking at the electronic densities. In an electric field energy is gained by moving the electronic densities in field direction. The  $1P_e(m \pm 1)$  densities shown in the bottom row of Fig. 3 can move quite freely in that direction with only a small increase in confining energy. Hence a strong dipole moment is induced leading to a pronounced Stark effect. On the other hand the cost in potential energy for the  $1P_e(m = 0)$  density by moving into the same direction is much higher due to the close confinement potential step. This leads to a smaller induced dipole moment as can be seen in the top row of Fig. 3, and therefore to a smaller quadratic Stark effect.

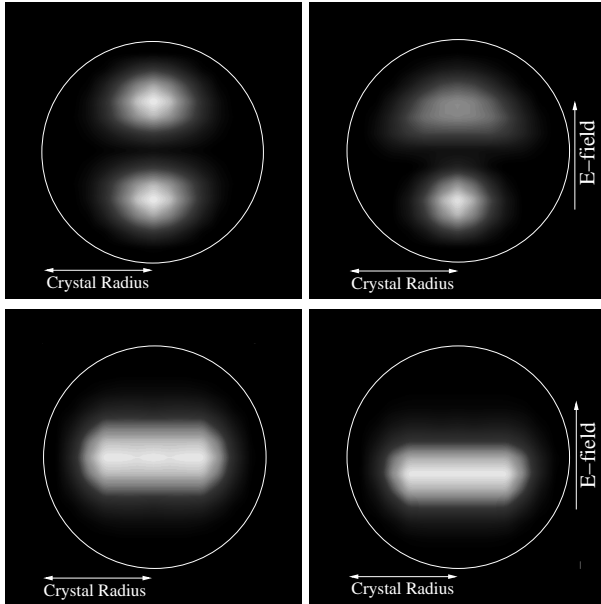


FIG. 3. Electronic density of the  $1P_e$  envelope wave functions calculated within a particle-in-a-sphere model. The densities illustrate qualitatively the different Stark effect on the  $1P_e$  state, although they were calculated in an infinite spherical well neglecting the non-parabolicity of the conduction band. Top and bottom left show the  $1P_e(m \pm 1)$  and  $1P_e(m = 0)$  densities without the presence of an electric field respectively. Whereas top right and bottom right show the corresponding densities in a homogeneous field of 0.18 V/nm

The quantitative tip-substrate voltage dependence of the  $1P_e$  energy level is shown in Fig. 2 for a QD radius of  $R_1 = 3.2$  nm. At an applied voltage of 1.4 V as used in experiment<sup>1</sup> the energetic difference between  $1P_e(m = 0)$  and  $1P_e(m \pm 1)$  is about 15 meV. This Stark induced energy splitting is experimentally resolvable and allows at an appropriate voltage tunneling into the ener-

getically lower  $1P_e(m \pm 1)$  states without tunneling into the  $1P_e(m = 0)$  state. The qualitatively different density distributions of those split states shown in Fig. 4 are observed in a STM experiment by Millo et. al.<sup>1</sup>. Therefore the obtained Stark induced degeneracy lifting of the first excited  $1P_e$  state serves as a possible explanation for experimentally observed mapping of the  $1P_e(m \pm 1)$  wave functions only (see discussion).

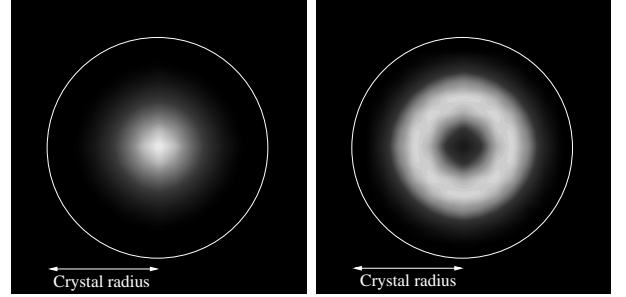


FIG. 4. The plots above show the electronic density of Fig. 3 viewed along the applied electric field. The  $1P_e(m = 0)$  density is shown left whereas on the right side the superposition of  $1P_e(m = 1)$  and  $1P_e(m = -1)$  is plotted.

#### IV. DISCUSSION

As shown in this publication the first  $1P_e$  electron will occupy one of the energetically lower  $1P_e(m \pm 1)$  states. The second electron is then going to occupy the other  $1P_e(m \mp 1)$  state. This leads to a torus like electron density seen in a wave function mapping experiment. Due to the exchange interaction the spins of both electrons line up.

If all  $1P_e$  states had been degenerate the third electron would have followed Hund's rule by occupying the  $1P_e(m = 0)$  state with same spin orientation as the first two electrons. This configuration shown on the left of Fig. 5 would have led to a spherical electronic density. But due to the Stark effect the  $1P_e$  degeneracy is now lifted such that configuration A competes with configuration B shown on the right of Fig. 5. This configuration would lead to a torus like electronic density since no electron is occupying the  $1P_e(m = 0)$  state.

In experiment<sup>1</sup> a torus like electron density was found with three electrons occupying the  $1P_e$  state, suggesting that configuration B has a smaller total energy.

Configuration A has to pay extra energy for the third electron due to the energetically higher  $1P_e(m = 0)$  level. On the other hand all spins are lined up such that this configuration takes advantage of the full exchange energy. In configuration B the situation is just opposite. While the third electron occupies the energetically lower  $1P_e(m = 1)$  level this configuration lacks the exchange energy of the third electron due to its reversed spin.

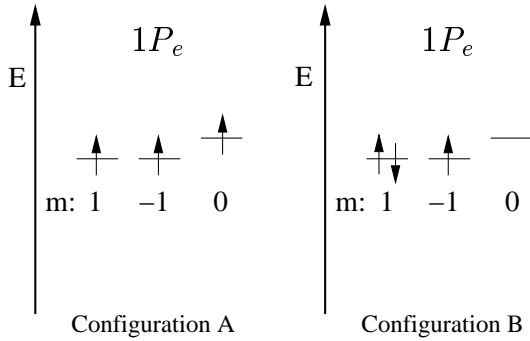


FIG. 5. Two possible configurations for three electrons in the  $1P_e$  states.

To find out which configuration has the lower energy, we calculate the contribution of the first order Coulomb interaction to the total energy. Using the wave function of a infinite spherical well we estimate that the exchange energy of configuration B is approximately 13 meV higher than in configuration A. This is 2 meV smaller than the Stark shift of A and therefore configuration B is favored, in agreement with experiment.

The first order Coulomb contribution for two electrons in the  $1S_e$  state yields a charging energy of 56 meV which is about half of the experimental value<sup>4</sup>. One reason for this small value is the neglected interaction with the polarization charges at the QD's surface. These charges induced by the electrons inside the QD are expected to be large due to the high dielectric mismatch at the surface. While this interaction enhances the charging energy, it has only a small effect on the exchange energy<sup>19</sup>.

Although our calculations explain the experimental data, the close competition between Stark effect and Coulomb interaction requires a more thorough investigation. On the one hand the actual electronic structure of the InAs/ZnSe nanocrystal, and on the other hand the influence of correlations on the Coulomb energy in these few electron systems has to be taken into account.

## V. CONCLUSION

We calculated the Stark effect perturbatively on the first excited CB state in an InAs nanocrystal within a particle-in-sphere model. An energy dependent effective mass was used to account for the non-parabolicity in the CB. The obtained degeneracy lifting of the first excited  $1P_e$  state provides a possible explanation for experimentally observed mapping of  $1P_e(m \pm 1)$  wave functions without  $1P_e(m = 0)$  mixing.

## ACKNOWLEDGMENTS

The authors gratefully acknowledge valuable discussions with Markus Morgenstern, Theophilos Maltezopoulos and Uri Banin. We would also like to thank Garnett

Bryant for kindly providing extended band calculations on InAs nanocrystals. This work was supported by the DFG through SFB 1641 and GrK 32048.

- 
- <sup>1</sup> O. Millo, D. Katz, Y. Cao, and U. Banin, Phys. Rev. Lett. **86**, 5751 (2001).
  - <sup>2</sup> B. Grandidier *et al.*, Phys. Rev. Lett. **85**, 1068 (2000).
  - <sup>3</sup> E. E. Vdovin *et al.*, Science **290**, 122 (2000).
  - <sup>4</sup> U. Banin, Y. Cao, D. Katz, and O. Millo, Letters to Nature **400**, 542 (1999).
  - <sup>5</sup> B. Alpers *et al.*, Applied Physics Letters **75**, 1751 (1999).
  - <sup>6</sup> G. W. Wen, J. Y. Lin, H. X. Jiang, and Z. Chen, Phys. Rev. B. **52**, 5913 (1995).
  - <sup>7</sup> S.-S. Li and J.-B. Xia, Journal of Applied Physics **88**, 7171 (2000).
  - <sup>8</sup> O. Millo, D. Katz, Y. Cao, and U. Banin, Phys. Rev. B. **61**, 16773 (2000).
  - <sup>9</sup> E. P. Backers and D. Vanmaekelbergh, Phys. Rev. B. **62**, 7743 (2000).
  - <sup>10</sup> D. J. Griffiths, *Introduction to Electrodynamics* (Prentice, Hall, 1998).
  - <sup>11</sup> O. Madelung, *Semiconductors-Basic Data*, 2nd revised ed. (Springer, Berlin, 1996).
  - <sup>12</sup> B. S. Kim, M. A. Islam, L. E. Brus, and I. P. Herman, Journal of Applied Physics **89**, 8127 (2001).
  - <sup>13</sup> L. Brus, Journal of Chemical Physics **80**, 4403 (1984).
  - <sup>14</sup> M. G. Burt, J. Phys.: Condens. Matter **4**, 6651 (1992).
  - <sup>15</sup> G. W. Bryant, *private communication*.
  - <sup>16</sup> For the infinite confinement potential the 2nd order perturbation theory has been compared to the results of a full diagonalization. The relative error of the perturbative calculation versus the full diagonalization is less than  $10^{-3}$  for voltages up to  $U = 2V$ .
  - <sup>17</sup> L. I. Schiff, *Quantum Mechanics* (Springer, Berlin, 1993).
  - <sup>18</sup> A. J. Williamson and A. Zunger, Phys. Rev. B. **59**, 15819 (1999).
  - <sup>19</sup> G. Goldoni *et al.*, Physica E **6**, 482 (2000).

TABLE I. This table shows the first two energy levels in an  $R_1 = 3.2$  nm InAs QD without an electric field. The energy difference between the ground and first excited states is in good agreement with experiment<sup>4</sup>.

State	Energy in meV	$E(1P_e) - E(1S_e)$
$1S_e$	542	
$1P_e$	861	319